THE JOURNAL OF BIOLOGICAL CHEMISTRY
Vol. 278, No. 42, Issue of October 17, pp. 40771–40777, 2003
Printed in U.S.A.

In Vivo Assembly of Phage φ29 Replication Protein p1 into Membrane-associated Multimeric Structures*

Received for publication, June 30, 2003, and in revised form, August 5, 2003
Published, JBC Papers in Press, August 6, 2003, DOI 10.1074/jbc.M306935200

Gemma Serrano-Heras‡, Margarita Salas§, and Alicia Bravo¶

From the Instituto de Biología Molecular Eladio Viñuela (CSIC), Centro de Biología Molecular Severo Ochoa (CSIC-UAM), Universidad Autónoma, Cantoblanco, 28049 Madrid, Spain

The mechanisms underlying compartmentalization of prokaryotic DNA replication are largely unknown. In the case of the *Bacillus subtilis* phage φ29, the viral protein p1 enhances the rate of *in vivo* viral DNA replication. Previous work showed that p1 generates highly ordered structures *in vitro*. We now show that protein p1, like integral membrane proteins, has an amphiphilic nature. Furthermore, immunoelectron microscopy studies reveal that p1 has a peripheral subcellular location. By combining *in vivo* chemical cross-linking and cell fractionation techniques, we also demonstrate that p1 assembles in infected cells into multimeric structures that are associated with the bacterial membrane. These structures exist both during viral DNA replication and when φ29 DNA synthesis is blocked due to the lack of viral replisome components. In addition, protein p1 encoded by plasmid generates membrane-associated multimers and supports DNA replication of a p1-lacking mutant phage, suggesting that the pre-assembled structures are functional. We propose that a phage structure assembled on the cell membrane provides a specific site for φ29 DNA replication.

In both eukaryotes and prokaryotes, the use of large organizing structures to bring together replication factors seems to be a general mechanism to enhance the efficiency of the replication process. In eukaryotes, chromosomal DNA replication occurs at numerous locations within the nucleus. Each site constitutes a replication factory containing many polymerizing machines working on different templates (1). Replication factories fixed to a nucleoskeleton have been visualized by electron microscopy techniques (2). This finding supports a replication model in which DNA polymerases are immobilized by attachment to larger structures, and DNA is pulled through (stationary replisome model) (3). Nuclear substructures also appear to have a central role in replication of DNA viruses, like the nuclear matrix in adenovirus DNA replication (4–6). Attachment of replication complexes to specific structures has also been reported for eukaryotic positive-strand RNA viruses. In this case, replication occurs in close association with intracellular membranes of diverse origin (*e.g.* endoplasmic reticulum, lysosome, chloroplast) (7). Furthermore, the discovery that chromosomal DNA replication in *Bacillus subtilis* and *Escherichia coli* takes place at a centrally located, stationary replication factory has led to the proposal that the bacterial replisome might be anchored to an underlying structure, presumably the bacterial membrane (8–10). However, despite these observations, little is known on the mechanisms that position the replication complexes at specific structures.

In the case of the *B. subtilis* phage φ29, cell fractionation studies showed that parental viral DNA-membrane complexes are formed near the onset of viral DNA replication. Moreover, formation of these complexes required the synthesis of early viral-encoded proteins (11). Thus, viral proteins appear to be involved in the attachment of φ29 DNA to the bacterial membrane. The genome of φ29 is a linear double-stranded DNA molecule with a terminal protein (TP)[1] covalently linked at each 5′-end. Its replication starts at either DNA end, where the replication origins are located, by a protein-priming mechanism. *In vitro*, this initiation mechanism requires the formation of a heterodimer between a free molecule of TP, which acts as a primer, and the φ29 DNA polymerase (12). The viral protein p1 (85 residues) enhances the rate of *in vivo* φ29 DNA replication, playing a critical role when bacteria are growing at high, rather than low, temperatures (13). Quantitative immunoblotting revealed that p1 is present in about 10^4 molecules per cell at early stages of infection, and it increases up to 10^5 molecules per cell at late stages (14). Protein p1 has interesting features such as the following. (i) It is recovered in membrane fractions of infected cells (14). (ii) It assembles into highly ordered structures *in vitro* (13), and (iii) its N-terminal region binds to primer TP *in vitro* (15). Although p1 has no sequence homology to cytoskeletal elements, we found that a truncated p1 protein that lacks the N-terminal 33 amino acids assembles *in vitro* into large polymers that show a parallel array of longitudinal protofilaments (13). These structures, examined by negative-stain electron microscopy, resemble polymers formed under particular *in vitro* conditions by FtsZ, which forms a ring-like structure that mediates bacterial cell division (16, 17). However, unlike FtsZ, p1 polymerization is not regulated by GTP hydrolysis. The ability of protein p1 to generate highly ordered structures *in vitro*, and its presence in membrane fractions of infected cells, led us to propose that p1 could assemble *in vivo* to form a multimeric structure in close association with the bacterial membrane. Verification of this hypothesis is essential to understand the role of p1 in φ29 DNA replication.

In this work, we show that p1, like integral membrane pro-

* This work was supported by Grants 2R01 GM27242-23 from the National Institutes of Health and PB98-0645 from the Dirección General de Investigación Científica y Técnica. The costs of publication of this article were defrayed in part by the payment of page charges. This article must therefore be hereby marked "*advertisement*" in accordance with 18 U.S.C. Section 1734 solely to indicate this fact.

‡ Recipient of a predoctoral fellowship from Ministerio de Ciencia y Tecnología (Spain).

§ To whom correspondence should be addressed. Tel.: 34-91-397-8435; Fax: 34-91-397-8490; E-mail: msalas@cbm.uam.es.

¶ Supported by the Ministerio de Ciencia y Tecnología (Programa Ramón y Cajal).

[1] The abbreviations used are: TP, terminal protein; BS^3, bis(sulfosuccinimidyl)suberate; Tricine, *N*-[2-hydroxy-1,1-bis(hydroxymethyl)ethyl]glycine.

teins (18), has an amphiphilic nature. Moreover, immunoelectron microscopy studies reveal that protein p1 is located at or close to the bacterial membrane. By combining *in vivo* chemical cross-linking and cell fractionation techniques, we also show that during ϕ29 DNA replication there are large homomeric p1 complexes associated with the bacterial membrane. Furthermore, protein p1 encoded by plasmid generates membrane-associated multimers and supports DNA replication of a p1-lacking mutant phage, suggesting that the pre-assembled structures are functional. We discuss the possible role of the p1 structures in the formation of ϕ29 DNA replication compartments.

EXPERIMENTAL PROCEDURES

Bacterial Strains, Bacteriophages, and Plasmids—*B. subtilis* 110NA, a non-suppressor (su^-) strain, and *B. subtilis* MO-99, a suppressor strain (su^{+3}), were used (19). The ϕ29 *sus*4 (56), *sus*3 (91) and *sus*2 (513) mutant phages were isolated by Moreno *et al.* (19). The ϕ29 *sus*1 (629) mutant phage was isolated by Reilly *et al.* (20). To construct plasmid pPR55.p1, a *Hinc*II-*Hinc*II DNA fragment from ϕ29 (coordinates 1447–850) (21), which contains the p1-encoding gene, was inserted into the T4 DNA polymerase-treated *Sph*I site of the *B. subtilis* expression vector pPR55 (22). Plasmid-containing cells were grown in LB medium (23) supplemented with phleomycin (0.8 μg/ml).

Phage Growth under One Step Conditions—Cultures were exponentially grown to ~10^8 cells/ml, and then infected at a multiplicity of infection of 5–10. After 10 min of incubation with gentle shaking, unadsorbed phages were eliminated by centrifugation of the infected culture. Cells were resuspended in the same volume of medium and incubated with vigorous shaking for the indicated time.

Synthesis of Viral DNA—The method used to measure synthesis of viral DNA under one step phage growth conditions was as described (22). Basically, total intracellular DNA was isolated at different times after infection, and analyzed by 0.8% agarose gel electrophoresis. Gels were stained with ethidium bromide. Images were obtained with the UVITec UV/WL 23 system. Bands corresponding to unit length ϕ29 DNA were quantified using the Image quant v1.1 program. The relative amount of viral DNA refers to the intensity of the intracellular ϕ29 DNA band with respect to that of proteinase K-treated ϕ29 DNA (50 ng) used as internal marker.

In Vivo Chemical Cross-linking—Bacteria were washed with 50 mM Hepes, pH 8.0, and concentrated 20-fold in buffer P (50 mM Hepes, 10 mM EDTA, 20% sucrose, pH 8.0). The cross-linker bis(sulfosuccinimidyl) suberate (BS^3) (Pierce) was dissolved in 50 mM Hepes, pH 8.0, just before use and added to the concentrated culture at different final concentrations. After incubation at room temperature for 20 min, Tris-HCl, pH 7.5, was added at a final concentration of 150 mM to quench the reaction.

Membrane Preparations—Membrane vesicles of *B. subtilis* cells were prepared as described (14). This method is based essentially on the procedure described by Konings *et al.* (24).

Triton X-114 Phase Partitioning—Triton X-114 is a non-ionic detergent with a low cloud point (23 °C) enabling protein solubilization with phase partitioning of hydrophilic from amphiphilic proteins (18). Cells were concentrated 4-fold in 50 mM glucose, 10 mM EDTA, 25 mM Tris-HCl, pH 8.0. Lysozyme was added at a final concentration of 120 μg/ml. After 10 min at room temperature, cells were sedimented by centrifugation. Detergent extraction of proteins was carried out overnight at 4 °C using 2% (v/v) Triton X-114 in phosphate-buffered saline (PBS) as described (25). Detergent-insoluble material was removed by centrifugation at 4 °C prior to phase separation. For phase partitioning, the sample was incubated at 37 °C for 10 min followed by centrifugation for 10 min at room temperature. The resulting aqueous and detergent phases were supplemented with Triton X-114 or PBS, respectively, and washed three times by repeating the phase separation step. Prior to SDS-Tricine-PAGE (26), proteins from the phases were precipitated with 10 volumes of acetone at −20 °C for 1 h.

Western Blots—Proteins were transferred electrophoretically to Immobilon-P membranes (Millipore) using either a Trans Blot apparatus (Bio-Rad) at 100 mA and 4 °C for 80 min, or a Mini Trans Blot (Bio-Rad) at 100 mA and 4 °C for 60 min. Transfer buffer contained 25 mM Tris, 192 mM glycine, 20% methanol. Membranes were probed with the indicated serum for 60 min. Antigen-antibody complexes were detected using anti-rabbit horseradish peroxidase-conjugated antibodies and ECL Western blotting detection reagents (Amersham Biosciences).

Affinity Purification of anti-p1 Antibodies—Protein p1 was transferred to Immobilon-P membranes, which were probed with anti-p1 serum for 16 h at 4 °C. Antibodies against p1 were eluted with 0.1 M glycine, pH 2.3. The eluted fraction was neutralized by adding 0.1 volume of 1 M Tris-HCl, pH 8.8.

Immunoelectron Microscopy—Cells were washed with Sörensen's buffer (0.1 M dibasic sodium phosphate, pH 7.2, 6% sucrose) and fixed with 4% paraformaldehyde, 0.1% glutaraldehyde in Sörensen's buffer at 4 °C for 4 h. Cells were cryoprotected with 15% glycerol, in 0.1 M dibasic sodium phosphate, pH 7.2, for 30 min and 30% glycerol, in 0.1 M dibasic sodium phosphate, pH 7.2, for 30 min. Then, cells were pelleted and immediately layered onto a sterile cellulose ester membrane filter (Whatman). Wedge-shaped portions of this filter were cryofixed by plunging into liquid propane in a KF80 cryofixation unit (Reichert Jung). Freeze substitution was performed with pure methanol containing 0.5% uranyl acetate in an automatic freeze-substitution unit (AFS, Leica) at −85 °C for 54 h. The temperature was gradually increased (5 °C/h) to −35 °C and held constant for 24 h. Samples were washed with pure methanol three times for 1 h each at −35 °C and then were infiltrated in a graded series of Lowicryl K4M/methanol mixtures (1:2 for 1 h, 1:1 for 2 h, 3:1 for 2 h). Cells were embedded in Lowicryl K4 M at −35 °C for 24 h and polymerized for 24 h under ultraviolet irradiation. During the polymerization step, the temperature was gradually increased to 22 °C. Infiltration, embedding, and polymerization steps were carried out in an automatic freeze-substitution equipment (AFS, Leica). Thin sections (70 nm) were obtained by cutting the specimen on a Reichert Jung ultracut E ultramicrotome and placed on collodion carbon-coated grids for immunogold labeling. Thin sections on the grids were blocked with TBS (30 mM Tris-HCl, pH 8.2, 150 mM NaCl) containing 5% bovine serum albumin (BSA) for 5 min. Then, they were incubated with affinity-purified p1 antibodies (diluted 1:10 in 0.1% acetylated BSA in TBS) for 1 h at room temperature. After three washes with 0.1% acetylated BSA in TBS, sections were incubated with 10 nm colloidal gold-labeled protein A (Biocell) (diluted 1:25 in 1% BSA in TBS) for 45 min. The grids were washed in TBS and double-distilled water and air-dried. Finally, sections were stained with 2% of aquous uranyl acetate for 7 min and 0.2% lead citrate for 25 s. Electron micrographs were taken in a Jeol 1010 electron microscope at 80 kV.

RESULTS

Protein p1 Has an Amphiphilic Nature—To perform experiments during *in vivo* viral DNA replication, *B. subtilis* non-suppressor (su^-) cells were infected with the ϕ29 *sus*4 (56) mutant phage. As shown in Fig. 1*A*, protein p1 and ϕ29 *sus*4 (56) DNA accumulated throughout the course of infection. At 30 min of infection, the intracellular level of p1 was similar to that previously measured in *B. subtilis* cells infected with the wild-type phage (14). In ϕ29 *sus*4 (56) infected cells, the ϕ29 regulatory protein p4 is not synthesized and, consequently, late viral transcription is not activated. The late genes encode components of the viral capsids, proteins involved in phage morphogenesis and those required for cell lysis (27). Hence, ϕ29 *sus*4 (56) DNA is replicated but it cannot be packaged into capsids.

The C-terminal sequence of p1 spanning residues Tyr^{68} to Ala^{84} is highly hydrophobic (Fig. 1*B*). Cell fractionation studies, performed with ϕ29 *sus*4 (56) infected cells, showed that p1 is recovered in membrane fractions during viral DNA replication (14). Unlike the wild-type p1, a truncated p1 protein that lacks the C-terminal 43 amino acids neither associates with membranes *in vivo* nor self-interacts *in vitro*, although it interacts with the primer TP *in vitro* (15). We have now investigated the nature of the association between protein p1 and membranes by phase partitioning with Triton X-114, a non-ionic detergent widely used for the isolation of integral membrane proteins. This technique accurately predicts membrane localization of proteins (18, 25). To this end, at 30 min of ϕ29 *sus*4 (56) infection, when viral DNA replication was taking place (Fig. 1*A*), whole cells were solubilized with Triton X-114, and the soluble material was subjected to phase separation. An immunoblot analysis of the aqueous and detergent phases using polyclonal antibodies against the viral proteins p1 and p6 is shown in Fig. 2. Protein p1 was found exclusively in the deter-

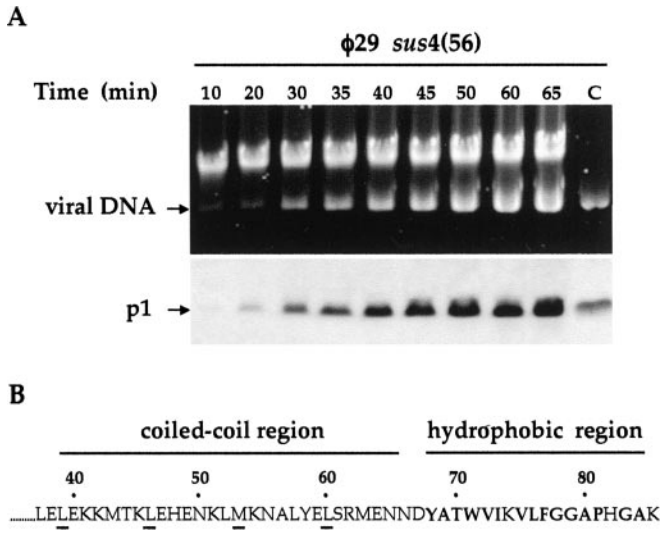

FIG. 1. *A*, time course of the accumulation of viral DNA and protein p1 under one step phage growth conditions. *B*, *subtilis* 110NA (*su*$^-$) cells growing in LB medium at 30 °C were infected with ϕ29 *sus*4 (56) mutant phage. Phage addition marked the zero time of the experiment. At the indicated times, aliquots were taken. *Upper part*, total intracellular DNA was isolated and analyzed by agarose-gel electrophoresis. The gel was stained with ethidium bromide. Proteinase K-treated ϕ29 DNA was run in the same gel as internal marker (*lane C*). *Lower part*, whole-cell extracts were prepared by sonication. Total proteins were separated by SDS-Tricine-PAGE (26) and analyzed by Western blotting using anti-p1 serum. Purified protein p1 was run in the same gel (*lane C*). *B*, amino acid sequence of p1 spanning residues Leu^{37} to Lys^{85}. The region that presumably forms an α-helical coiled-coil structure is shown. Leu and Met residues of the heptad repeat units are underlined. The hydrophobic segment at the C terminus is indicated.

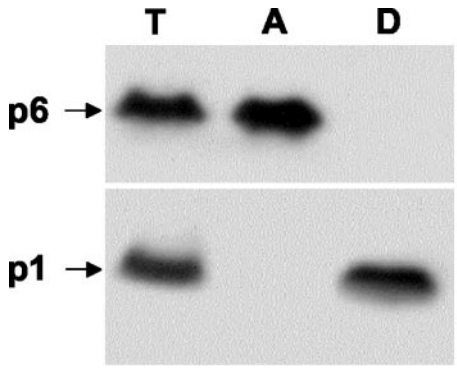

FIG. 2. **Amphiphilic nature of protein p1.** *B. subtilis* 110NA (*su*$^-$) cells growing in LB medium at 30 °C were infected with ϕ29 *sus*4 (56). Triton X-114 was used to solubilize whole cells. Solubilized proteins (*T*) and proteins recovered in the aqueous (*A*) and detergent (*D*) phases were separated by SDS-Tricine-PAGE and analyzed by immunoblotting using polyclonal antibodies against p1 and p6.

gent phase, whereas the hydrophilic protein p6, used as a control, was recovered in the aqueous phase. The nucleoid-associated protein p6 is essential for *in vivo* viral DNA replication (28). Thus, this biochemical analysis shows that p1 has an amphiphilic nature, suggesting that it associates with membranes as an integral protein.

Peripheral Location of p1 in Infected Cells by Immunoelectron Microscopy—In a complementary approach to localize p1 in infected cells, we used immunoelectron microscopy. To increase the signal of p1, cells were fixed and processed for immunolabeling at 45 min of ϕ29 *sus*4 (56) infection. At this time, the intracellular level of p1 was ~3-fold higher than at 30 min, and synthesis of viral DNA was still taking place (see Fig. 1*A*). Cell sections were incubated with affinity-purified p1 antibodies and then incubated with colloidal gold-labeled protein A. As control, non-infected cells were processed. In both infected and non-infected cells, 1800 cross-sections on different grids were examined. In infected cells, 38.4% of the sections had one, two, or three gold particles (Fig. 3*A*). This percentage was 3.3-fold higher than in non-infected cells. In addition, the number of gold particles counted was 4.1-fold higher in infected than in non-infected cells. We also determined the number of gold particles located at cytoplasm and periphery on the cross-sections (Fig. 3*B*). Gold particles at the membrane and within ~35 nm of the membrane were scored as being at the periphery. The most noticeable feature of the distribution of label was the high number of gold particles at the periphery of infected cell sections (out of 899 particles counted, 690 were at the periphery). This distribution reflects the positioning of p1, because in non-infected sections, out of 219 particles counted, 102 were at the periphery. Thus, the ratio between peripheral and cytoplasmic gold particles was 3.8-fold higher in infected than in non-infected cells. Cross-sections of infected cells with peripheral gold particles are shown in Fig. 3*C*. These results indicate that protein p1 is located at or near the cell membrane, rather than being randomly dispersed, and are consistent with its copurification with membranes on cell fractionation (14).

Protein p1 Forms Membrane-associated Multimeric Structures during in Vivo Viral DNA Replication—Protein p1 was shown to be able to self-interact into highly ordered structures *in vitro* (13). The COILS prediction program (29) revealed that the region of p1 spanning residues Glu^{38} and Asn^{65} has a high probability (0.98) of forming a α-helical coiled-coil structure (Fig. 1*B*). Such a sequence functions to assemble an N-terminal truncated p1 protein (p1ΔN33) into two-dimensional sheets (30). To investigate whether p1 assembles *in vivo* into multimers that associate with the bacterial membrane, we carried out *in vivo* chemical cross-linking experiments followed by cell fractionation. At 30 min of ϕ29 *sus*4 (56) infection (see Fig. 1*A*), cells were incubated with different concentrations of BS^3. This homobifunctional cross-linker reacts significantly with the ϵ-amine of lysine residues, which are frequent in p1 (12 residues out of 85). Following this treatment, membrane fractions were obtained by a method that yields almost exclusively "right-side-out" membrane vesicles (24). Total proteins from the membrane preparations were separated by denaturing polyacrylamide gel electrophoresis and analyzed by immunoblotting using anti-p1 serum (Fig. 4). As control, membrane preparations from non-infected cells were analyzed. The anti-p1 serum cross-reacted with a host membrane-associated protein that migrated at ~50 kDa (protein X). This protein provided an internal control of specificity in the cross-linking reaction. In infected cells and in the absence of BS^3, a product migrating as the p1 monomer (8.5 kDa) was detected. At low concentrations of BS^3 (0.25–0.5 mM), two products migrating at 18 kDa and 30 kDa appeared (referred to as II and III in Fig. 4). These products are likely cross-linked p1 dimers and trimers, respectively, taking into account the MW of the BS^3 cross-linker (572.43 Da). At 2 mM BS^3, cross-linked p1-containing material that migrates between 43 kDa and 203 kDa was also detected. According to the regular pattern, they are presumably p1 homo-complexes. At 5 mM BS^3, the p1 monomeric form was not detected, and the amount of p1 complexes smaller than 70 kDa drastically decreased. This decrease correlated with an increase in the amount of higher molecular weight complexes, which were specific of infected cells. Thus, we conclude that protein p1 assembles *in vivo* into large membrane-associated multimers. These multimeric structures are present during viral DNA replication.

Assembly of p1 into Membrane-associated Multimers Also Occurs in the Absence of Viral Components—The ϕ29 replisome

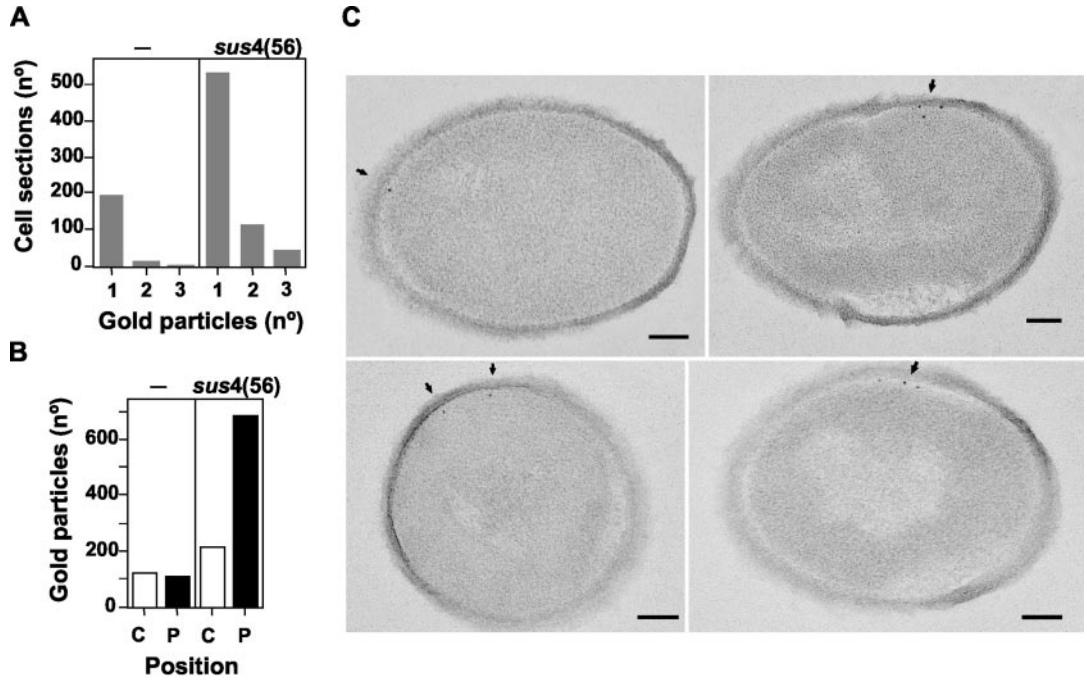

FIG. 3. **Localization of protein p1 in ϕ29 *sus*4 (56) infected cells by immunoelectron microscopy.** Affinity-purified p1 antibodies were used. *A*, number of cross-sections with one, two, or three gold particles. *B*, cellular distribution of the gold particles. *C*, cytoplasm; *P*, periphery. *C*, immunoelectron micrographs of cross-sections from infected cells. Gold particles at the cell periphery are indicated by *arrows*. The bar equals 100 nm.

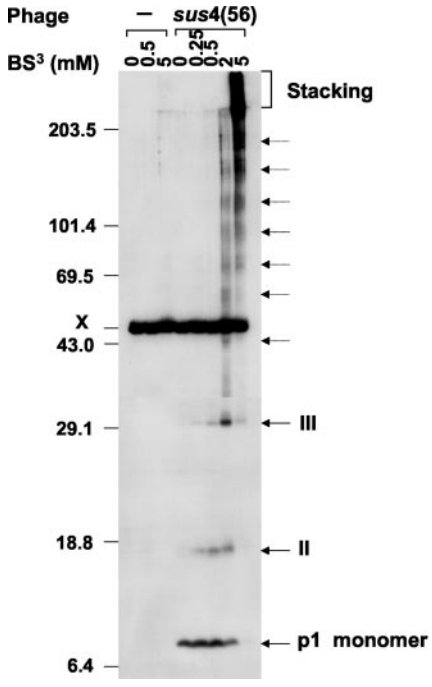

FIG. 4. **Membrane-associated p1 multimers in infected cells.** *B. subtilis* 110NA (*su*$^-$) cells growing in LB medium at 30 °C were infected with ϕ29 *sus*4 (56). After 30 min, cells were incubated with the indicated concentration of BS^3. Total proteins from the membrane fractions were separated by SDS-PAGE (10–20% polyacrylamide gradient). The gel was processed for immunoblotting using anti-p1 serum. The molecular mass of prestained proteins used as markers is indicated on the *left* in kilodaltons. The *arrows* on the right show the position of cross-linked p1 complexes.

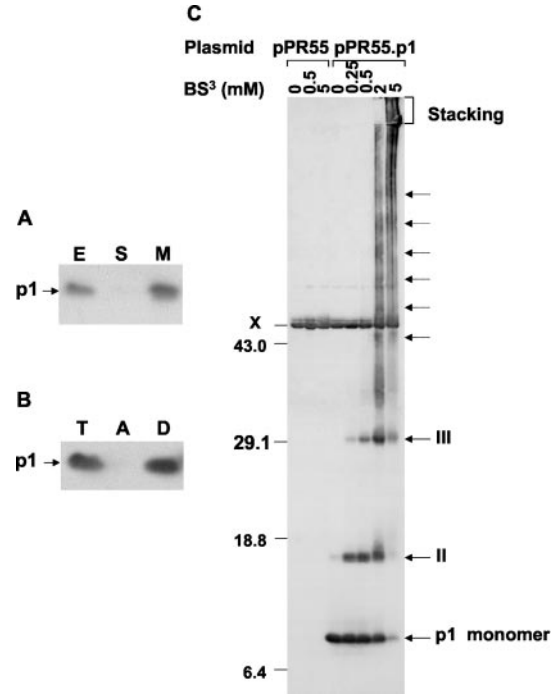

FIG. 5. **Membrane-associated p1 multimers in cells carrying plasmid pPR55.p1.** *B. subtilis* 110NA (*su*$^-$) cells carrying pPR55.p1 were grown in LB medium at 37 °C. *A*, whole-cell extracts were prepared and fractionated. Equivalent amounts of extract (*E*), soluble fraction (*S*), and membrane fraction (*M*) were analyzed by immunoblotting. *B*, immunoblot analysis after extraction of pPR55.p1-carrying cells with Triton X-114. *T*, solubilized material; *A*, aqueous phase; *D*, detergent phase. *C*, immunoblot analysis of membrane fractions from plasmid-containing cells treated with BS^3. See legend to Fig. 4.

is constituted at least by a free molecule of the TP (primer protein) and the ϕ29 DNA polymerase. *In vitro* studies showed that this heterodimer interacts with the ends of the genome, where the replication origins are located. Then, replication starts by a protein-priming mechanism in which the ϕ29 DNA polymerase catalyzes the linkage of dAMP to the primer TP (12). We have analyzed whether membrane-associated p1 multimers are formed when initiation of *in vivo* ϕ29 DNA synthesis is blocked. To this end, *B. subtilis su*$^-$ cells were infected with the ϕ29 *sus*2 (513) mutant phage. Under these conditions,

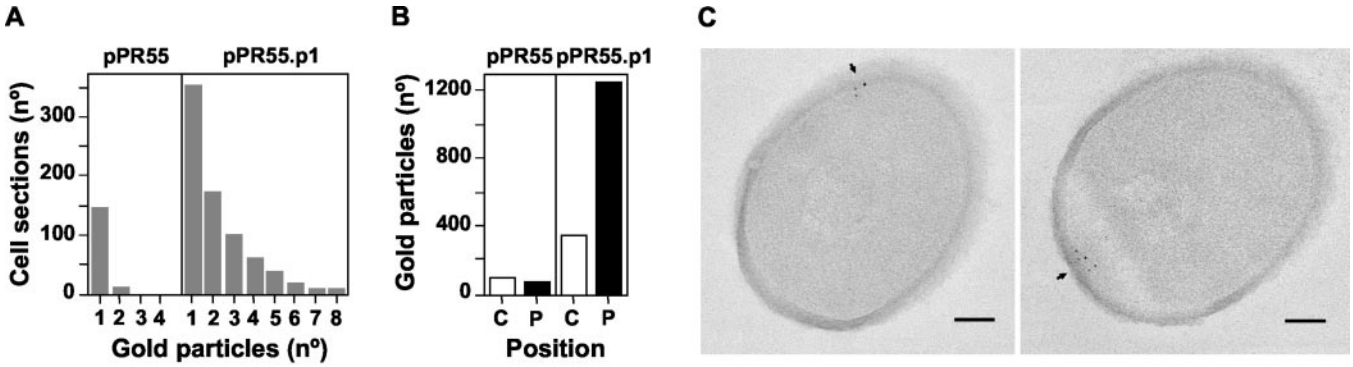

FIG. 6. **Localization of p1 in pPR55.p1-carrying cells by immunoelectron microscopy.** Affinity-purified p1 antibodies were used. *A*, histogram of the number of cross-sections with the indicated number of gold particles. *B*, number of gold particles found at the indicated position. *C*, cytoplasm; *P*, periphery. *C*, immunoelectron micrographs of cross-sections from cells carrying pPR55.p1. The *bar* equals 100 μm.

initiation of phage DNA replication is blocked due to the lack of the ϕ29 DNA polymerase. After 30 min of infection, cells were treated with BS^3 and then fractionated. Immunoblot analysis of the membrane fractions using anti-p1 serum showed a pattern of cross-linked p1 complexes (not shown) similar to that observed during viral DNA replication (Fig. 4). The same result was obtained when *B. subtilis* su^- cells were infected with the ϕ29 *sus*3 (91) mutant phage (not shown). In this case, ϕ29 DNA synthesis is blocked due to the lack of the primer TP. Thus, membrane-associated p1 multimers are also assembled in the absence of viral replisome components.

We next studied whether other viral components are required for the formation of membrane-associated p1 multimers. To this end, the p1-encoding gene was inserted into the constitutive expression vector pPR55 (plasmid pPR55.p1). The amount of p1 was ~2-fold higher in cells carrying the recombinant plasmid than in 45 min ϕ29 *sus*4 (56) infected cells, as determined by immunoblotting (not shown). When pPR55.p1-carrying cells were fractionated, p1 was recovered in the membrane fraction (Fig. 5*A*). Moreover, after extraction with Triton X-114, p1 was exclusively found in the detergent phase (Fig. 5*B*). We also examined whether p1 formed multimeric structures by treatment of pPR55.p1-carrying cells with BS^3. Cells harboring pPR55 were used as control. Fig. 5*C* shows an immunoblot analysis of the membrane fractions using anti-p1 serum. In pPR55.p1-carrying cells, the pattern of cross-linked p1 complexes was indistinguishable from that observed in ϕ29 *sus*4 (56) infected cells (Fig. 4). Immunoelectron microscopy studies using affinity-purified p1 antibodies confirmed the peripheral location of p1 in pPR55.p1-carrying cells (Fig. 6). Again, cells harboring pPR55 were used as control. In both cases, 1800 cross-sections on different grids were examined. In vector-carrying cells, only 8.5% of the sections were labeled, and 164 gold particles were counted (Fig. 6*A*). In pPR55.p1-carrying cells, the percentage of labeled sections increased 4.8-fold. Moreover, the total number of gold particles increased 9.7-fold. Most of the labeled sections (83.3%) had one, two, or three gold particles, although sections with 4 to 8 gold particles were also found. Fig. 6*B* shows the distribution of the gold particles on the cross-sections. In vector-carrying cells, out of the 164 particles counted, 69 were at the periphery, whereas in pPR55.p1-carrying cells, out of the 1596 particles counted, 1252 were at the periphery. Thus, the ratio between peripheral and cytoplasmic gold particles was 5-fold higher in pPR55.p1-containing cells. Cross-sections of pPR55.p1-carrying cells with peripheral gold particles are shown in Fig. 6*C*.

Trans-complementation Mediated by Protein p1—Taken together, the above results indicated that protein p1 encoded by plasmid is able to assemble into membrane-associated multimers. If these p1 structures were similar to those assembled in

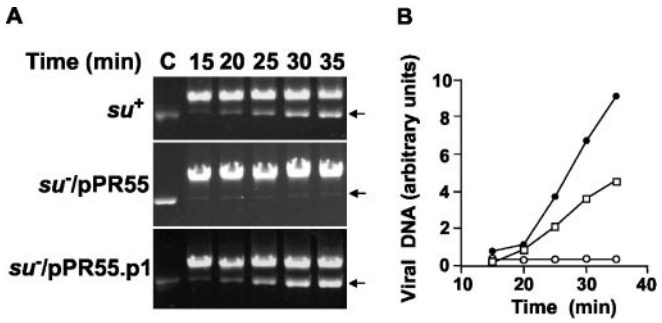

FIG. 7. **Trans-complementation mediated by p1.** *A*, synthesis of viral DNA under one step phage growth conditions. The indicated *B. subtilis* strains, grown in LB medium at 37 °C, were infected with ϕ29 *sus*1 (629). At the indicated times, total intracellular DNA was isolated and analyzed by agarose gel electrophoresis. Proteinase K-treated ϕ29 DNA was run in the same gel (*lane C*). The arrows show the position of ϕ29 DNA. *B*, kinetics of accumulation of ϕ29 *sus*1 (629)-DNA in su^+ (□); su^-/pPR55 (○), and su^-/pPR55.p1 (●) cells. The quantification corresponds to the gels shown in *A*.

infected cells, we reasoned that they should support replication of a p1-lacking mutant phage. To assess this prediction, we analyzed replication of the ϕ29 *sus*1 (629) mutant phage in different genetic backgrounds: plasmid-free suppressor (su^+) cells and non-suppressor (su^-) cells carrying either pPR55 or pPR55.p1 (Fig. 7). When pPR55-carring su^- cells were infected with the ϕ29 *sus*1 (629) mutant phage, no synthesis of viral DNA was detected. In contrast, phage DNA replication took place in pPR55.p1-carrying su^- cells. In these cells, the kinetics of accumulation of viral DNA was even faster than that obtained in su^+ cells infected with the *sus*1 (629) mutant, and the amount of viral DNA accumulated at 35 min was ~2-fold higher. Hence, these results suggest that the membrane-associated p1 structures formed in pPR55.p1-carrying cells are functional *in trans*.

DISCUSSION

Assembly of p1 into Membrane-associated Multimeric Structures—A remarkable finding of this study is that protein p1 of phage ϕ29 assembles *in vivo* into large multimeric structures. Furthermore, these structures interact with the bacterial membrane, as supported by the following results. (i) Protein p1 has an amphiphilic nature, as determined by Triton X-114 phase partitioning. (ii) p1 copurifies with membranes on cell fractionation (14), and (iii) immunoelectron microscopy studies show that p1 has a peripheral subcellular location.

In infected cells, membrane-associated p1 structures exist both when viral DNA replication takes place and when initiation of ϕ29 DNA synthesis is blocked due to the lack of viral replisome components. Membrane-associated p1 structures are

also generated in cells harboring a p1-encoding plasmid, indicating that their formation does not require other viral components. The ability of p1 to self-associate has also been demonstrated *in vitro*. For example, protein p1 functions as a polymerization domain when it is fused to the maltose-binding protein, leading to the formation of long filamentous structures (13). In addition, a truncated p1 protein that lacks the N-terminal 33 amino acids self-interacts into two-dimensional protofilament sheets. This assembly is mediated by a short α-helical coiled-coil sequence (30). The coiled-coil motif is also the main structural element in eukaryotic lamins, a class of nuclear intermediate filament proteins (31, 32). *In vivo*, different lamin proteins form the nuclear lamina, a thin fibrous structure immediately underlying the inner nuclear membrane of most eukaryotic cell nuclei (33). It remains to be determined what kind of structures p1 would form *in vivo*.

Role of the Membrane-associated p1 Structures in ϕ29 DNA Replication—Parental ϕ29 DNA-membrane complexes have been isolated from infected cells. Formation of these complexes, which were detected near the onset of viral DNA replication, required the synthesis of early ϕ29-encoded proteins (11). Our present results support an *in vivo* replication model in which a p1 structure assembled on the bacterial membrane provides a specific site for ϕ29 DNA replication (15). According to this model, the ϕ29 DNA replication machinery, constituted at least by the primer TP-ϕ29 DNA polymerase heterodimer, would be targeted to the membrane-associated p1 structure. This association could be achieved by protein-protein interactions between protein p1 and primer TP, since the N-terminal 42 amino acid residues of p1 are sufficient for binding to the primer TP *in vitro* (15). Once ϕ29 DNA replication starts by a protein-priming mechanism, the primer TP remains covalently bound to the newly synthesized DNA and thereby, viral DNA becomes membrane-associated when it is replicated. This compartmentalization model also accounts for the presence of p1, primer TP and ϕ29 DNA polymerase in membrane fractions of infected cells when initiation of phage DNA replication is blocked due to the lack of the nucleoid-associated protein p6 (14).

The role proposed for the membrane-associated p1 structure resembles the function of the eukaryotic nuclear matrix in adenovirus DNA replication. Like phage ϕ29, the genome of adenovirus is a linear double-stranded DNA with a TP covalently attached to each 5′-end. Therefore, its replication proceeds via a protein-priming mechanism (34). Cell fractionation studies indicated that adenovirus DNA is tightly bound to the nuclear matrix throughout the course of infection (35, 36). It has been shown that this attachment is mediated by the TP covalently bound to the DNA (37). Furthermore, the precursor of the TP, which interacts with the viral DNA polymerase and primes DNA replication, binds to the nuclear matrix both *in vivo* and *in vitro* (4). Hence, the nuclear matrix is thought to provide the structural framework on which the replication factors and DNA can bind and interact.

Comparison with other Viral Systems—Replication of eukaryotic viral genomes does not occur randomly in the infected cell but is localized to specific sites. Replication of most DNA viruses occurs within the cell nucleus. In this case, nuclear substructures seem to be involved in the formation of DNA replication compartments (5, 6, 38). For example, as mentioned above, adenovirus replicates at distinct subnuclear sites on the nuclear matrix (39, 40). In the case of positive-strand RNA viruses, the docking to specific intracellular membranes seems to be essential for the assembly of active replication complexes. Membranes appear to function not just as a way of compartmentalizing virus RNA replication, but also appear to have a central role in the organization and function of the replication machinery (7). Some progress has been made in understanding how the viral RNA replication apparatus is fixed to specific types of membranes. In Semliki Forest virus, binding of the viral replicase to endosomal/lysosomal membranes is likely mediated by the RNA-capping protein Nsp1, which has affinity for negatively charged phospholipids (41, 42). Moreover, the tobacco etch potyvirus 6-kDa protein is thought to be necessary for targeting viral RNA replication complexes to endoplasmic reticulum-derived membranes. This protein associates with membranes as an integral protein via a 19 amino acid hydrophobic domain (43). In contrast to those viruses, a host-encoded protein seems to act as a membrane anchor of the tobamoviruses replication complexes. This protein associates with membranes and interacts with the helicase domain of virus-encoded replication proteins (44). In poliovirus, electron microscopy revealed that purified RNA-dependent RNA polymerase forms planar and tubular oligomeric arrays. In addition, membranous vesicles isolated from infected cells contain structures consistent with the presence of two-dimensional polymerase arrays on their surfaces during infection (45).

Therefore, as it happens in eukaryotic viral genomes, replication of the *B. subtilis* phage ϕ29 occurs at specific subcellular localizations. We suggest that the p1 structure assembled on the cell membrane provides an anchoring site for the ϕ29 replication complexes.

Acknowledgments—We thank M. T. Rejas for help with immunoelectron microscopy. The institutional help of Fundación Ramón Areces to the Centro de Biología Molecular "Severo Ochoa" is acknowledged.

REFERENCES

1. Newport, J., and Yan, H. (1996) *Curr. Opin. Cell Biol.* **8,** 365–368
2. Hozák, P., Hassan, A. B., Jackson, D. A., and Cook, P. R. (1993) *Cell* **73,** 361–373
3. Cook, P. R. (1999) *Science* **284,** 1790–1795
4. Fredman, J. N., and Engler, J. A. (1993) *J. Virol.* **67,** 3384–3395
5. Bridge, E., and Petterson, U. (1995) *Curr. Top. Microbiol. Immunol.* **199,** 99–117
6. Lamond, A. I., and Earnshaw, W. C. (1998) *Science* **280,** 547–553
7. Buck, K. W. (1996) *Adv. Virus Res.* **47,** 159–251
8. Lemon, K. P., and Grossman, A. D. (1998) *Science* **282,** 1516–1519
9. Koppes, L. J., Woldringh, C. L., and Nanninga, N. (1999) *Biochimie* (*Paris*) **81,** 803–810
10. Lemon, K. P., and Grossman, A. D. (2000) *Mol. Cell* **6,** 1321–1330
11. Ivarie, R. D., and Pène, J. J. (1973) *Virology* **52,** 351–362
12. Salas, M., Miller, J. T., Leis, J., and DePamphilis, M. L. (1996) in *DNA Replication in Eukaryotic Cells* (DePamphilis, M. L., ed) pp. 131–176, Cold Spring Harbor Laboratory Press, Cold Spring Harbor, NY
13. Bravo, A., and Salas, M. (1998) *EMBO J.* **17,** 6096–6105
14. Bravo, A., and Salas, M. (1997) *J. Mol. Biol.* **269,** 102–112
15. Bravo, A., Illana, B., and Salas, M. (2000) *EMBO J.* **19,** 5575–5584
16. Erickson, H. P., Taylor, D. W., Taylor, K. A., and Bramhill, D. (1996) *Proc. Natl. Acad. Sci. U. S. A.* **93,** 519–523
17. Rothfield, L. I., and Justice, S. S. (1997) *Cell* **88,** 581–584
18. Bordier, C. (1981) *J. Biol. Chem.* **256,** 1604–1607
19. Moreno, F., Camacho, A., Viñuela, E., and Salas, M. (1974) *Virology* **62,** 1–16
20. Reilly, B. E., Zeece, V. M., and Anderson, D. L. (1973) *J. Virol.* **11,** 756–760
21. Yoshikawa, H., and Ito, J. (1982) *Gene* (*Amst.*) **17,** 323–335
22. Bravo, A., Hermoso, J. M., and Salas, M. (1994) *Mol. Gen. Genet.* **245,** 529–536
23. Sambrook, J., Fritsch, E. F., and Maniatis, T. (1989) *Molecular Cloning: A Laboratory Manual*, 2nd Ed., Vol. 3, A.1, Cold Spring Harbor Laboratory, Cold Spring Harbor, NY
24. Konings, W. N., Bisschop, A., Veenhuis, M., and Vermeulen, C. A. (1973) *J. Bacteriol.* **116,** 1456–1465
25. Brusca, J. S., and Radolf, J. D. (1994) *Methods Enzymol.* **228,** 182–193
26. Schagger, H., and Jagow, G. (1987) *Anal. Biochem.* **166,** 368–379
27. Salas, M., and Rojo, F. (1993) in *Bacillus subtilis and other Gram-positive Bacteria: Biochemistry, Physiology, and Molecular Genetics* (Sonenshein, A. L., Hoch, J. A., and Losick, R., eds) pp. 843–857, American Society for Microbiology, Washington, D. C.
28. Carrascosa, J. L., Camacho, A., Moreno, F., Jiménez, F., Mellado, R. P., Viñuela, E., and Salas, M. (1976) *Eur. J. Biochem.* **66,** 229–241
29. Lupas, A. (1996) *Trends Biochem. Sci.* **21,** 375–382
30. Bravo, A., Serrano-Heras, G., and Salas, M. (2001) *J. Biol. Chem.* **276,** 21250–21256
31. Aebi, U., Cohn, J., Buhle, L., and Gerace, L. (1986) *Nature* **323,** 560–564
32. Herrmann, H., and Aebi, U. (2000) *Curr. Opin. Cell Biol.* **12,** 79–90
33. Moir, R. D., Spann, T. P., Lopez-Soler, R. I., Yoon, M., Goldman, A. E., Khuon, S., and Goldman, R. D. (2000) *J. Struct. Biol.* **129,** 324–334
34. de Jong, R. N., and van der Vliet, P. C. (1999) *Gene* (*Amst.*) **236,** 1–12
35. Younghusband, H. B., and Maundrell, K. (1982) *J. Virol.* **43,** 705–713

36. Bodnar, J. W., Hanson, P. I., Polvino-Bodnar, M., Zempsky, W., and Ward, D. C. (1989) *J. Virol.* **63,** 4344–4353
37. Schaack, J., Ho, W. Y., Freimuth, P., and Shenk, T. (1990) *Genes Dev.* **4,** 1197–1208
38. Verheijen, R., Van Venrooij, W., and Ramaekers, F. (1988) *J. Cell Science* **90,** 11–36
39. Pombo, A., Ferreira, J., Bridge, E., and Carmo-Fonseca, M. (1994) *EMBO J.* **13,** 5075–5085
40. Angeletti, P. C., and Engler, J. A. (1998) *J. Virol.* **72,** 2896–2904
41. Ahola, T., Lampio, A., Auvinen, P., and Kääriäinen, L. (1999) *EMBO J.* **18,** 3164–3172
42. Lampio, A., Kilpeläinen, I., Pesonen, S., Karhi, K., Auvinen, P., Somerharju, P., and Kääriäinen, L. (2000) *J. Biol. Chem.* **275,** 37853–37859
43. Schaad, M. C., Jensen, P. E., and Carrington, J. C. (1997) *EMBO J.* **16,** 4049–4059
44. Yamanaka, T., Ohta, T., Takahashi, M., Meshi, T., Schmidt, R., Dean, C., Naito, S., and Ishikawa, M. (2000) *Proc. Natl. Acad. Sci. U. S. A.* **97,** 10107–10112
45. Lyle, J. M., Bullitt, E., Bienz, K., and Kirkegaard, K. (2002) *Science* **296,** 2218–2222

In Vivo Assembly of Phage φ29 Replication Protein p1 into Membrane-associated Multimeric Structures

Gemma Serrano-Heras, Margarita Salas and Alicia Bravo

J. Biol. Chem. 2003, 278:40771-40777.
doi: 10.1074/jbc.M306935200 originally published online August 6, 2003
